Xanthine Oxidase–Dependent Regulation of Hypoxia-Inducible Factor in Cancer Cells

Corinne E. Griguer,[1] Claudia R. Oliva,[1] Eric E. Kelley,[2] Gregory I. Giles,[2] Jack R. Lancaster, Jr.,[2] and G. Yancey Gillespie[1]

Departments of [1]Surgery, [2]Anesthesiology, Physiology and Biophysics, and Environmental Health Sciences, and Center for Free Radical Biology, University of Alabama at Birmingham, Birmingham, Alabama

Abstract

During chemical hypoxia induced by cobalt chloride ($CoCl_2$), hypoxia-inducible factor 1α (HIF1-α) mediates the induction of a variety of genes including erythropoietin and vascular endothelial growth factor. We used glioma cells with oxidative phosphorylation–dependent (D54-MG) and glycolytic-dependent (U251-MG) phenotypes to monitor HIF1-α regulation in association with redox responsiveness to $CoCl_2$ treatment. We showed that $CoCl_2$ increased xanthine oxidase (XO)–derived reactive oxygen species (ROS), which causes accumulation of HIF1-α protein in U251-MG cells. Under these conditions, blockade of XO activity by pharmacologic (*N*-acetyl-L-cysteine or allopurinol) or molecular (by small interfering RNA) approaches significantly attenuated HIF1-α expression. Exogenous H_2O_2 stabilizes HIF1-α protein. XO was present in these cells and was the primary source of free radicals. We also showed higher XO activity in cells exposed to $CoCl_2$ compared with cells grown in normoxia. From the experiments shown here, we concluded that ROS were indeed generated in D54-MG cells exposed to $CoCl_2$ but it was unlikely that ROS participated in the hypoxic signal transduction pathways in this cell type. Possibly, cell type–dependent and stimulus-dependent factors may control ROS dependency or redox sensitivity of HIF1-α and thus HIF1-α activation either directly or by induction of specific signaling cascades. Our findings reveal that XO-derived ROS is a novel and critical component of HIF1-α regulation in U251-MG cells, pointing toward a more general role of this transcription factor in tumor progression. (Cancer Res 2006; 66(4): 2257-63)

Introduction

Hypoxia results in the coordinated up-regulation of numerous genes involved in glucose transport, glycolysis, erythropoiesis, and angiogenesis, which is mediated by the hypoxia-inducible factor 1α (HIF1-α; refs. 1, 2). Whereas HIF1-α protein is expressed at low levels due its rapid degradation, it is accumulated following hypoxic stress through inhibition of its proteosomal degradation (3). Interestingly, exposure to cobalt chloride ($CoCl_2$) triggers transcriptional changes that mimic the hypoxic response, including up-regulation of HIF1-α, erythropoietin, and glycolytic enzymes (4–6). Although it has been well documented that $CoCl_2$ can cause stabilization of HIF1-α, the biochemical mechanism by which $CoCl_2$ accomplishes this remains unknown. One model suggested that the hydroxylation of HIF1-α is mediated by a group of HIF-specific hydroxylases and that $CoCl_2$ can inactivate the enzymes by occupying an iron-binding site on the proline hydroxylases (7, 8). One common mechanism that may underlie hypoxia and $CoCl_2$-induced changes in gene expressions is the increased generation of reactive oxygen species (ROS; ref. 9), providing a redox signal for HIF1-α induction (5, 10, 11). Generation of ROS during hypoxia as well as in the presence of $CoCl_2$ has been described (5, 9, 12). However, the role of ROS in the activation of HIF1-α is not clear (1, 9, 13). It has been proposed (5, 14–17) that hypoxia activates transcription via mitochondria-dependent signaling process involving increased ROS whereas $CoCl_2$ activates transcription by stimulating ROS generation via a mitochondria-independent mechanism. Minchenko et al. (18) have proposed that the integrity of the mitochondrial respiratory chain is not necessary for hypoxia response. Furthermore, they show that H_2O_2 is not an intermediary molecule involved in oxygen sensing. Salnikow et al. (13) concluded that ROS are produced during exposure of cells to metals that mimic hypoxia but the formation of ROS was not involved in the activation of HIF1-α–dependent genes. These results prompted us to reevaluate the role of ROS in HIF-1 activation. Recently, we have described specific bioenergetic markers associated with the metabolic phenotype of several human and mouse glioma cell lines. We hypothesized that glioma cells would express one of at least two different metabolic phenotypes, possibly acquired through progression. The D54-MG and GL261 glioma cell lines displayed an oxidative phosphorylation–dependent phenotype and, alternatively, U251-MG and U87-MG glioma cells exhibited a glycolytic-dependent phenotype with functional oxidative phosphorylation (19). These observations raised the possibility that the heterogeneity in glucose metabolism might identify an important biological marker of glioma cells that is critical for their progression and adaptation to hypoxic conditions. The present study used glioma cells with oxidative phosphorylation–dependent and glycolytic-dependent phenotypes as prototype cells to test whether HIF1-α levels in glioma cells are regulated by ROS.

We used a pharmacologic and molecular approach to show xanthine oxidase (XO)–dependent or XO-independent pathway of HIF1-α induction in U251-MG or D54-MG cells, respectively. These results revealed a novel role of XO in cancer pathogenesis as well as in oxygen-regulated cellular physiology. To our knowledge, this is the first report showing that XO is involved in the regulation of HIF1-α.

Materials and Methods

Cell lines, cultures, and chemicals. Human glioma cell lines U251-MG and D54-MG were originally obtained from Dr. D.D. Bigner (Duke

Note: C.E. Griguer and C.R. Oliva have contributed equally to this work.
In memory of R. Griguer.

Requests for reprints: Corinne E. Griguer, Department of Surgery, University of Alabama at Birmingham, 1918 University Boulevard, THT 1046, Birmingham, AL 35294-0005. Phone: 205-934-7227; E-mail: cgriguer@uab.edu.

doi:10.1158/0008-5472.CAN-05-3364

University, Durham, NC). All cell lines were cultured using a 50:50 mixture of DMEM and Ham's nutrient mixture F12 (MediaTech, Herdon, VA) supplemented with 7% heat-inactivated fetal bovine serum (HyClone, Logan, UT) and 2.6 mmol/L L-glutamine. All chemicals were obtained from Sigma Chemical Co. (St. Louis, MO) unless otherwise stated.

Nuclear extracts and immunoblot analysis. Nuclear and cytosolic fractions were isolated using NE-PER Nuclear and Cytoplasmic Extraction Reagents according to the instructions of the manufacturer (Pierce, Rockford, IL). Western blot analyses were done as previously described (19). Anti-HIF1-α antibody was purchased from Transduction Laboratories (Lexington, KY) and anti-XO antibody was from Rockland, Inc. (Gilbertsville, PA). Western blots were quantified by densitometry using Scion Image (version 4.02, Scion Corp., Frederick, MD).

Measurements of ROS and reduced glutathione/oxidized glutathione. Intracellular ROS generation was assessed by using 2′,7′-dichlorofluorescin diacetate (DCFH-DA; Molecular Probes). D54-MG and U251-MG cells at 50% confluence were incubated with DCFH diacetate (10 μmol/L) for 5 hours with or without $CoCl_2$. The media were removed, the cells were lysed and centrifuged to remove debris, and the fluorescence was measured (excitation, 500 nm; emission, 530 nm). Data were normalized to the control (without $CoCl_2$) values. Reduced glutathione (GSH) and oxidized glutathione (GSSG) were determined using Bioxytech GSH/GSSG-412 kit according to the instructions of the manufacturer (OxisResearch, Portland, OR).

Electron paramagnetic resonance spectrometry and spin trapping. Electron paramagnetic resonance (EPR) measurements were done using a Bruker Elexsys E-500 spectrometer equipped with an ER049X microwave bridge and an AquaX cell. Studies were done using the following variables: 40 mW microwave power, 100 kHz modulation frequency, 1 G modulation amplitude, 3510 G center field, 100 G sweep width, 164 ms time constant, 168 seconds sweep time, 60 dB receiver gain, and 1024 data points. The constituents 5,5-dimethyl-1-pyrroline-*N*-oxide (DMPO; 25 mmol/L), allopurinol (150 μmol/L), and xanthine (50 μmol/L) were added to a cell suspension (10×10^6-12×10^6 cells/mL in PBS, pH 7.4) and the spectrum recorded after 10 minutes. Adventitial metals were eliminated from all buffers by treatment with Chelex resin.

Measurement of XO activity. For measurement of XO activity, cell lysates were prepared according to Zweier et al. (20). Lysates were spectrophotometrically assayed at 290 nm for uric acid production in the presence of 60 μmol/L xanthine as previously described (21). Enzyme activity is expressed in microunits per milligram of protein, where 1 unit of activity equals 1 μmol of substrate converted to uric acid per minute.

Small interfering RNA. Adherent cells were transfected with small interfering RNA (siRNA) as follows: cationic lipid complexes were formed with 1 μmol/L siRNA oligonucleotides in combination with 3 μL of *trans*IT siQuest Transfection Reagent (Mirus, Madison, WI) in 0.25 mL of OPTI-MEM (Invitrogen, Carlsbad, CA) and added to six-well plates containing 1.25 mL of complete medium per well. Cells were maintained in culture for 48 hours. siRNAs specific for XO (SMART pool XO, accession number NM_000379) and control scrambled siRNAs were obtained from Dharmacon, Inc. (Lafayette, CO). Transfection efficiency was >80% as determined by fluorescent-labeled control siRNA (Mirus) according to the instructions of the manufacturer.

Results

HIF1-α is rapidly activated in response to $CoCl_2$ in U251-MG and D54-MG Cells. $CoCl_2$ has been used extensively to study the hypoxic signaling pathway because of the hypoxia-mimicking effect under normoxic conditions. Throughout the present study, 100 μmol/L $CoCl_2$ was used as a hypoxia-mimetic reagent for no more than 5 hours. Over 95% of the cells excluded trypan blue, indicating that cell viability was not compromised during $CoCl_2$ treatment. We first examined the time course for $CoCl_2$ induction of HIF1-α protein levels in our two models (Fig. 1). Cells were treated with $CoCl_2$ for the indicated times and HIF1-α

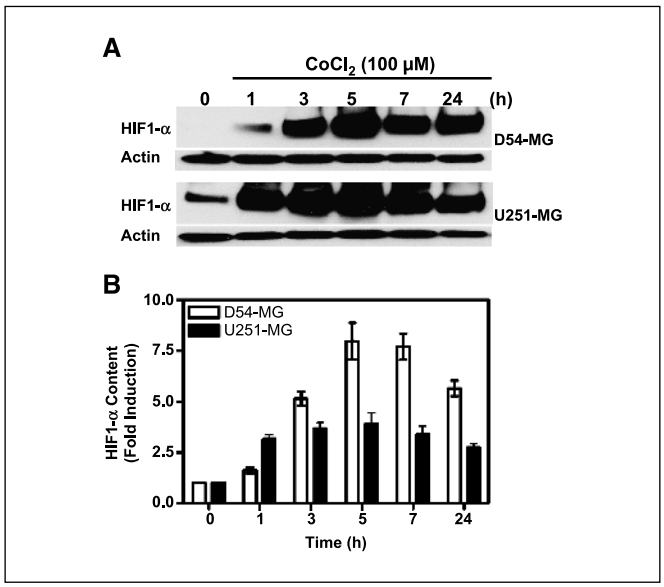

Figure 1. Effects of $CoCl_2$ treatments on nuclear abundance of HIF1-α. *A,* time-dependent variations in HIF1-α nuclear abundance as assessed by immunoblotting showing protein abundance with $CoCl_2$ treatment. β-Actin is shown as an internal reference for semiquantitative loading in each lane. *B,* the percentage relative maximal abundance of HIF1-α against that obtained under control conditions without $CoCl_2$ treatment. *Columns,* mean of the relative intensity of the bands from four independent experiments; *bars,* SD.

was measured by Western blot (Fig. 1*A*). HIF1-α protein expression increased in both cell lines when exposed to $CoCl_2$ for up to 24 hours with a maximum reaching 5 hours (Fig. 1). However, the profile of HIF1-α induction showed some differences between cell lines. A 3-fold increase of HIF1-α expression was detected as early as 1 hour of exposure to $CoCl_2$ in U251-MG, with a maximum of 4-fold induction detected at 5 hours (Fig. 1*B*). On the other hand, HIF1-α induction in D54-MG showed a 1.6-fold increase within the first hour follow by an 8-fold maximum increase induction within 5 to 7 hours. The level of HIF1-α protein expression in U251-MG cells under control conditions seems to be elevated in comparison with D54-MG, suggesting different mechanisms of HIF1-α regulation under normoxic conditions in both cell lines.

Requirement of ROS for induction of HIF1-α expression. Intracellular ROS generation was examined in human D54-MG and U251-MG glioma cells in response to $CoCl_2$ using DCFH-DA (21). Previous studies have indicated that DCFH oxidation can be mediated by H_2O_2 but not by superoxide (22). 2′,7′-Dichlorofluorescein (DCF) fluorescence was assessed under normoxia (21% O_2) in the presence of $CoCl_2$ for 5 hours. Both cell lines exhibited increases in DCF fluorescence during $CoCl_2$ treatment (Fig. 2*A*).

To assess whether $CoCl_2$ acts as a negative buffer of the glutathione pool, concentrations of GSH and GSSG were determined in extracts from control cultures and from cultures treated with $CoCl_2$ for 5 hours. GSH/GSSG ratios were also determined for each cell line as useful measure of oxidative stress. GSH concentration in D54-MG was higher than in U251-MG (688 versus 291 μmol/L, respectively) under control conditions. Consequently, the initial GSH/GSSH ratio is 2-fold higher in D54-MG cells compared with U251-MG cells. When cells were treated with $CoCl_2$, GSH/GSSG ratio decreased 2-fold in D54-MG whereas it remained unchanged in U251-MG. For U251-MG cells, this ratio

was equivalent to the values determined for D54-MG after $CoCl_2$ treatment. These results strongly suggest that these two cell lines possess different redox environments and have different buffering capabilities against ROS generation by $CoCl_2$. However, we cannot exclude other lines of antioxidant defense within U251-MG cells, such as vitamin E, β-carotene, and coenzyme Q or enzymatic antioxidant defenses, including catalases, peroxidases, superoxide dismutases, and glutathione *S*-transferases (23, 24).

HIF1-α induction is reduced by *N*-acetyl-L-cysteine. *N*-Acetyl-L-cysteine (NAC) has the capacity to decrease electrophiles and thus acts as a potent antioxidant with cytoprotective potential. In addition to its direct antioxidant effects, NAC may also serve as a precursor for cysteine and glutathione biosynthesis, thereby increasing the cellular pool of nucleophilic species (25). Thus, we tested whether NAC was able to abrogate HIF1-α induction in both cell lines. Figure 2*B* illustrates the variation in nuclear protein abundance of $CoCl_2$ induction of HIF1-α after NAC pretreatment (16 hours, 0-40 mmol/L). HIF1-α induction in D54-MG was maintained for concentrations up to 20 mmol/L NAC whereas for higher concentrations up to 40 mmol/L, a significant increase was observed. By contrast, HIF1-α induction in U251-MG was significantly abrogated in a dose-dependent manner. Figure 2*C* represents the densitometric analysis of HIF1-α abundance in both cell lines normalized to β-actin [*, $P < 0.05$; **, $P < 0.01$, as compared with cultures without pretreatment (0 mmol/L NAC)]. NAC induced a significant, dose-dependent increase in HIF1-α nuclear abundance in D54-MG, which was greater at higher doses of NAC tested (30 or 40 mmol/L). These observations suggest that NAC pretreatment effectively manipulated the cobalt/redox-dependent signaling sequence, which governs nuclear abundance of HIF1-α. In contrast, the induction of HIF1-α was substantially inhibited by NAC in U251-MG in a dose-dependent manner. The maximum inhibition was evident with 30 mmol/L NAC whereas even the lowest concentration tested (5 mmol/L) showed mild, but significant, attenuation of HIF1-α (Fig. 2*C*).

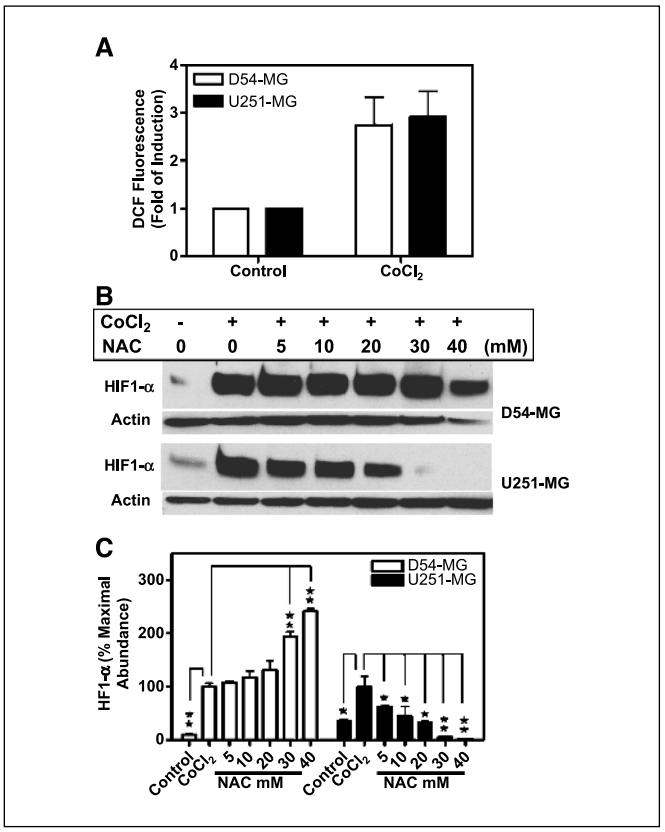

Figure 2. *A,* DCF fluorescence as a measure of ROS generation. Cells were incubated with DCFH-DA (10 μmol/L) for 30 minutes in the presence or absence of $CoCl_2$ (100 μmol/L). Results are expressed relative to control conditions without $CoCl_2$. *Columns,* mean of the relative DCF fluorescence from three independent experiments; *bars,* SD. *B* and *C,* effects of NAC pretreatments on nuclear abundance of HIF1-α under $CoCl_2$ treatment. *B,* dose-dependent variations in HIF1-α nuclear abundance were assessed by immunoblotting for protein abundance after treatment with different concentrations of NAC. β-Actin is shown as an internal reference for semiquantitative loading in each lane. *C,* relative abundance of HIF1-α compared with that obtained under activating conditions (100 μmol/L $CoCl_2$) without NAC pretreatment. *, $P < 0.05$; **, $P < 0.01$; ***, $P < 0.001$, as compared with control. *Columns,* mean of the relative intensity of the bands from four independent experiments; *bars,* SD.

XO inhibitors block cobalt-induced HIF1-α protein in U251-MG cells but not in D54-MG. The mitochondrial electron transport chain, the NADPH oxidase complex, and XO are potentially involved in mechanisms of ROS generation, and by extension, in mechanisms that stabilize HIF1-α protein in response to $CoCl_2$. To define the relative role of each system, we used inhibitors of NAD(P)H oxidase, electron transport chain, or XO to determine the effect on $CoCl_2$-induced HIF1-α protein levels in both glioma cell lines. Diphenylene iodonium inhibits electron transport in flavin-containing systems including NAD(P)H oxidase and mitochondrial complex I (26). Complex I inhibitors such as rotenone have been shown to inhibit the stabilization of HIF1-α protein, presumably by blocking the electron flow proximal to mitochondrial complex III, thereby ablating ROS generation (15, 27). Allopurinol and its major metabolite oxypurinol are purine analogues that form a tight-binding complex with molybdenum at the active site of XO, leading to the inhibition of its activity (28). Here, we assessed the role of these different ROS blockers in HIF1-α induction by $CoCl_2$ in both cell lines.

Cells untreated or pretreated for 1 hour with diphenylene iodonium (1 μmol/L), allopurinol (1 mmol/L), or rotenone (1 μmol/L) were exposed to $CoCl_2$. Figure 3*A* illustrates a representative immunoblot with the different blockers. HIF1-α induction by $CoCl_2$ in D54-MG was insensitive to rotenone, allopurinol, or diphenylene iodonium, suggesting a ROS-independent pathway of HIF1-α induction. By contrast, in U251-MG cells, allopurinol, a specific XO competitive inhibitor, abrogated 90% of HIF1-α induction by $CoCl_2$ (Fig. 3*B*). Intracellular ROS generation was examined in response to $CoCl_2$. U251-MG and D54-MG cells incubated with $CoCl_2$ showed an increase in DCF fluorescence. The increase in DCF fluorescence induced by $CoCl_2$ was abolished by pretreatment with allopurinol in U251-MG cells. By contrast, rotenone and diphenylene iodonium failed to attenuate the $CoCl_2$-stimulated increase in DCF signal (Fig. 3*C*). As expected, rotenone, allopurinol, or diphenylene iodonium did not alter the $CoCl_2$-stimulated increase in DCF fluorescence in D54-MG cells. These results support the hypothesis that ROS generated through XO is required for stabilization of HIF1-α in U251-MG glioma cells in response to $CoCl_2$ but not in D54-MG cells.

Measurement of cellular XO activity in glioma cells. Both ROS generation experiments and inhibition of HIF1-α induction by allopurinol provided evidence that XO was an important source of radical generation and may be relevant in the signaling pathway involving the HIF1-α induction in U251-MG cells. Although XO activity has been determined in a number of animal tumors and in a few human tumors (29–37), little is known about the expression

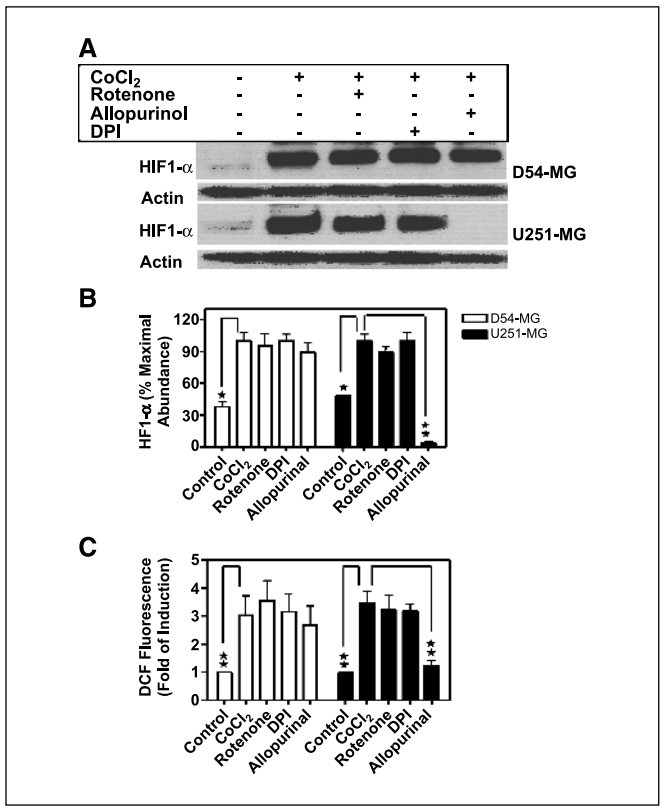

Figure 3. Effects of ROS inhibitors on nuclear abundance of HIF1-α under $CoCl_2$ treatment. Cells were incubated with the indicated blockers for 1 hour, followed by addition of $CoCl_2$ for 5 hours. *A,* HIF1-α nuclear abundance was assessed with immunoblotting to show changes in protein abundance with different ROS blockers. β-Actin is shown as an internal reference for semiquantitative loading in each lane. *B,* relative abundance of HIF1-α protein compared with that obtained with 100 μmol/L $CoCl_2$ with or without inhibitor pretreatment. *, $P < 0.05$; **, $P < 0.01$, as compared with control. *Columns,* mean of the relative intensity of the bands from six independent experiments; *bars,* SD. *C,* DCF fluorescence as a measure of ROS generation with different ROS blockers. *, $P < 0.05$; **, $P < 0.01$, as compared with control. *Columns,* mean of four independent experiments; *bars,* SD.

of XO in cancer cells. Therefore, experiments were done to determine whether or not D54-MG and U251-MG cells contained measurable XO activity and whether or not XO activity is increased in glioma cells treated with $CoCl_2$. As shown in Fig. 4*A* and *B*, XO activity was $\sim 139 \pm 13$ and 166 ± 7 microunits mg^{-1} for D54-MG and U251-MG, respectively, at untreated baseline conditions. Allopurinol decreased XO activity in a dose-dependent manner in both cell lines. Thus, there is measurable XO activity in these human glioma cells. In addition, $CoCl_2$ induced a significant increased in XO activity (1.4- and 1.6-fold of increase for D54-MG and U251-MG, respectively), suggesting an enzymatic activation by $CoCl_2$ treatment. In the presence of allopurinol, a >90% reduction in the enzymatic activity was observed compared with that in the absence of the blocker (Fig. 4*A* and *B*). To further evaluate the basis for the increased XO activity, we examined the effect of $CoCl_2$ on the amount of XO protein. As determined by Western blot, the amount of XO protein relative to total cellular protein remained constant after $CoCl_2$ exposure for up to 5 hours (data not shown).

Measurements of free radical generation. XO has been hypothesized to be an important source of free radical generation in cells and tissues; however, it is unknown if this enzyme is a significant source of radical generation in human tumor cells. To address this question, U251-MG cells subjected to $CoCl_2$ treatment were harvested, washed, and resuspended in PBS with the addition of xanthine and 2,2-dimethoxypropane (DMP). The cells were immediately transferred to an EPR with liquid sample cell and spectra were acquired. EPR signals consisting of a prominent 1:2:2:1 quartet signal indicative of DMPO-OH adduct were observed (Fig. 4*B*). To further confirm that XO was the source of free radical generation, similar experiments were done in the presence of allopurinol. In the presence of allopurinol, a >95% reduction in the magnitude of the DMPO-OH signals was observed compared with that in the absence of the blocker. These studies suggest that XO-derived radical generation occurs and is an important mechanism of radical generation in these cells.

Exogenous peroxide increases HIF1-α protein. The observation that NAC and allopurinol abolished HIF1-α induction by $CoCl_2$ suggests that H_2O_2 acts as a signaling element in this response. Therefore, exogenous administration of H_2O_2 should stabilize HIF1-α during normoxia. To produce a more sustained elevation in H_2O_2 levels, U251-MG cells were treated with repeated doses of H_2O_2 every 10 minutes for 2 hours. This approach was sufficient to trigger the stabilization of HIF1-α protein levels for low H_2O_2 concentrations (50, 100, and 300 μmol/L). However, exogenous administration of higher doses of H_2O_2 (0.5 and 1 mmol/L) abolished stabilization of HIF1-α in a dose-dependent manner (Fig. 4*C*).

XO-specific siRNA blocked $CoCl_2$-induced stabilization of HIF1-α. Because expression of HIF1-α was suppressed by allopurinol during the $CoCl_2$ induction, we investigated the effects of XO-specific siRNAs on HIF1-α stabilization by $CoCl_2$. As illustrated in Fig. 5*A*, transfection of XO siRNA suppressed by $64 \pm 11\%$ the expression of XO as compared with cells transfected with scrambled siRNA. To determine the effects of $CoCl_2$ on ROS generation in siRNA-transfected cells, DCF fluorescence was assessed in the presence of 100 μmol/L $CoCl_2$. Scramble-transfected cells exhibited increases in DCF fluorescence during $CoCl_2$ treatment and allopurinol abolished the increase in DCF fluorescence. In contrast, XO siRNA blocked ROS production in response to $CoCl_2$ (Fig. 5*B*). Figure 5*C* and *D* shows the effects of silencing XO on the expression of HIF1-α induction by $CoCl_2$. When XO-siRNA–transfected U251-MG cells were exposed to $CoCl_2$, a significant decrease (>75%) in HIF1-α induction was observed. On the other hand, in U251-MG cells transfected with scrambled siRNA, $CoCl_2$ significantly increased HIF1-α induction. These results indicate that suppression of XO expression is associated with a decrease of ROS production and HIF1-α induction.

Discussion

The present investigation revealed a novel signaling pathway mediating the effect of $CoCl_2$ on HIF1-α stabilization and nuclear translocation. ROS have been proposed to participate in the signal transduction process mediating the stabilization of HIF1-α during chemical hypoxia by $CoCl_2$. However, controversy exists about whether ROS levels increase or decrease under chemical hypoxia. The present study shows that HIF1-α stabilization by $CoCl_2$ requires an increase in ROS in U251-MG cells. Inhibition of $CoCl_2$-induced expression of HIF1-α by NAC indicated that redox-sensitive mechanisms were involved in this signaling pathway. Because $CoCl_2$ induced ROS production in U251-MG cells and NAC attenuated this response, it is tempting to speculate that ROS

contributed to activation of HIF1 by $CoCl_2$. Finally, H_2O_2 caused HIF1-α stabilization under normoxic conditions in U251-MG cells. Indeed, U251-MG cells responded to low H_2O_2 concentrations (0.05-0.3 mmol/L) by accumulation of HIF1-α. However, higher H_2O_2 doses (0.5-1 mmol/L) abolished HIF1-α induction. These observations indicate that low levels of an oxidizing stimulus are sufficient to stabilize HIF1-α. These results are consistent with previous reports showing that H_2O_2 bolus treatment in Hep3B and 293 cells induced the accumulation of HIF1-α (15). Collectively, these findings support the conclusion that ROS are both required and sufficient to activate the signaling system resulting in the stabilization of HIF1-α in U251-MG cells. Our findings are consistent with previous reports showing that chemical hypoxia induced increases in ROS generation in cancer cells (13).

The concept has been put forward that ROS events are master regulators of HIF1-α; however, the precise signaling pathway implicated awaits clarification. To identify the site of ROS generation in U251-MG cells, mitochondrial electron transport chain inhibitors were administered during $CoCl_2$ treatment. Mitochondrial complex III can generate ROS especially in the presence of compounds that prolong the half-life of ubisemiquinone (38, 39). Therefore, mitochondrial electron transport chain inhibitors that suppress the formation of ubisemiquinone at complex III should abolish the induction of HIF1-α seen during $CoCl_2$ treatment. However, neither of the complex I inhibitors, rotenone or diphenylene iodonium, abolished the HIF1-α induction. These results show that ROS generation at complex III is not required for the induction of HIF1-α during $CoCl_2$ treatment. Because diphenylene iodonium also inhibits flavoprotein oxidases (26), including NAD(P)H oxidase and cytochrome *P*450 reductase, we concluded that cytochrome *P*450 or NAD(P)H oxidase does not participate in the induction of HIF1-α during $CoCl_2$ treatment in U251-MG cells. Although increased ROS production in response to $CoCl_2$ has been previously attributed to a nonmitochondrial mechanism (5), the site(s) of other sources of ROS has not been determined. Our data suggest that XO is important in this process because inhibiting this enzyme with allopurinol completely abolished $CoCl_2$ induction of HIF1-α in U251-MG cells. XO has been hypothesized to be an important source of free radicals in postischemic cells and tissue (40); however, cultured human cells generally do not express XO when cultured in normoxia. Nevertheless, SV40 immortalized human mammary epithelial cell line (HB4a; ref. 41) and isolated human aortic endothelial cells (20) showed measurable XO activity and this enzyme was a significant source of radical generation. We observed that the addition of xanthine to U251-MG cells previously exposed to $CoCl_2$ led to a greater production of ROS than in cells not exposed to $CoCl_2$. This xanthine-dependent production of free radicals was completely blocked with allopurinol, confirming that the free radical source was the XO system. The concentrations of allopurinol that we used in this study are comparable to other studies and indicated that allopurinol did not act as a nonspecific scavenger of either superoxide or hydroxyl radicals (20). Thus, XO seemed to be a novel and essential component of HIF1-α regulatory machinery in U251-MG. Further experiments were done to determine whether this XO-mediated radical generation was triggered by increased enzyme activity. We observed in human glioma cells U251-MG and D54-MG that there is a significant XO activity that can be measured by the spectrophotometric assay of urate formation and that XO activity is increased during $CoCl_2$ treatment without changes in XO protein levels. A recent report suggests a hypoxic activation of xanthine oxidoreductase in BEAS-2B cells; however, the authors were not able to show XO activation by $CoCl_2$. The authors suggest that the signaling pathway involving the HIF1-α transcription factor may

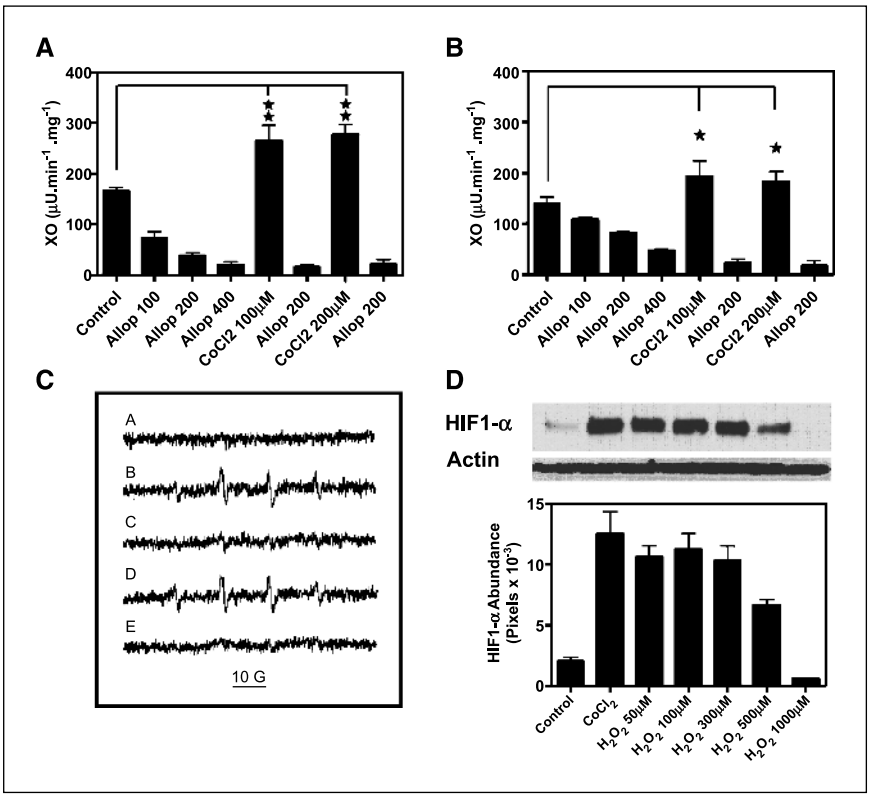

Figure 4. *A* and *B,* effect of $CoCl_2$ and allopurinol on XO activity. Lysates of untreated cultures of glioma cells or those exposed to $CoCl_2$ 100 μmol/L for 5 hours (*A,* U251-MG; *B,* D54-MG) were used to measure XO activity in the presence or absence of different concentrations of allopurinol. *Columns,* mean of specific XO activity from four independent experiments; *bars,* SD. *C,* XO-dependent cellular radical production. U251-MG human glioma cell suspensions (10×10^6-12×10^6 cells/mL in PBS, pH 7.4) were incubated with DMPO (25 mmol/L) and indicated quantities of XO substrate/inhibitor and radical production were assessed by EPR spectroscopy as described in Materials and Methods. *A,* spectrum of control cells plus DMPO in the absence of xanthine. *B,* control cells plus DMPO and xanthine (50 μmol/L). *C,* control cells plus DMPO, xanthine (50 μmol/L), and allopurinol (150 μmol/L). *D,* cobalt-treated cells plus DMPO and xanthine (50 μmol/L). *E,* cobalt-treated cells plus DMPO, xanthine (50 μmol/L), and allopurinol (150 μmol/L). *D,* effect of H_2O_2 on HIF1-α induction. U251-MG cells were exposed to repeated dosed of H_2O_2 (0.05-1 mmol/L) every 10 minutes for 2 hours. *Top,* HIF1-α nuclear abundance was assessed by immunoblotting, showing protein abundance with different H_2O_2 concentrations. β-Actin is shown as an internal reference for semiquantitative loading in each lane. *Bottom,* densitometric analysis of HIF1-α induction. *Columns,* mean of the relative intensity of the bands from three independent experiments; *bars,* SD.

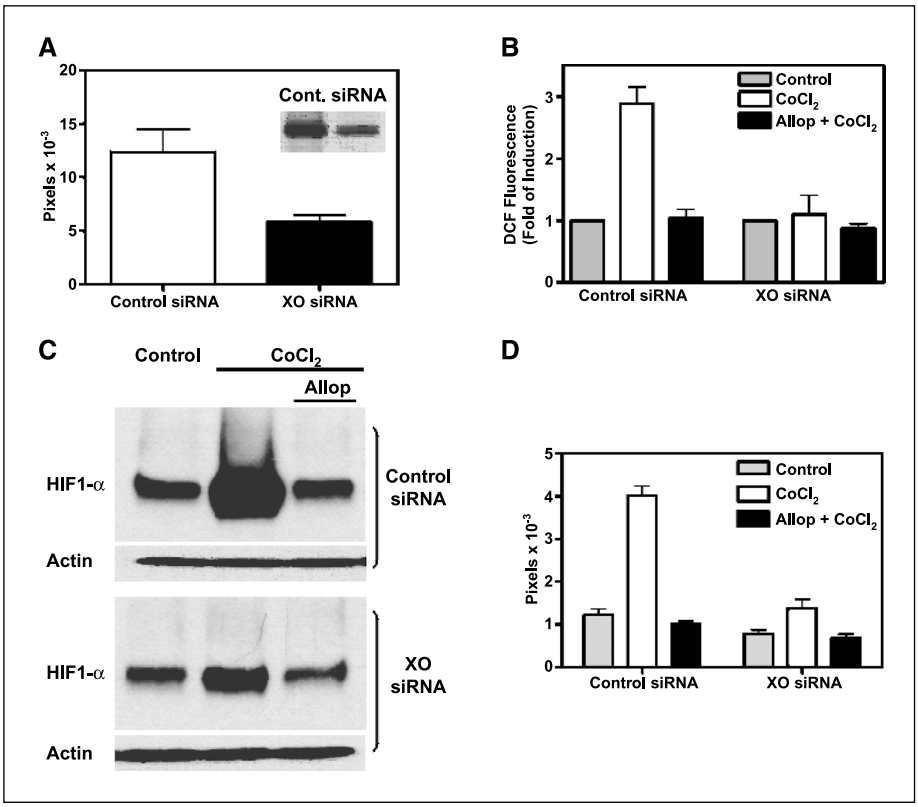

Figure 5. Down-regulation of XO expression by siRNA transfection. *A,* Western blot analysis showing the effects of XO-siRNA or control-siRNA transfections on expression of XO. *B,* effect of $CoCl_2$ and allopurinol on ROS generation in XO-siRNA– or control-siRNA–transfected cells. *C,* effect of $CoCl_2$ and allopurinol on HIF1-α induction in XO-siRNA– or control-siRNA–transfected cells. *D,* densitometric analysis of HIF1-α induction presented in (*B*). *Columns,* mean of the relative intensity of the bands from three independent experiments; *bars,* SD.

not be relevant (42). The discrepancy with our results may be due to cell type–specific responses or variations in experimental conditions. It is important to note that in the results reported by Linder et al. (42), the cells were incubated with $CoCl_2$ for 24 hours. Our results showed that $CoCl_2$ stimulation transiently elevated HIF1-α protein levels, peaking at 3 to 4 hours, consistent with the idea that a rapid increase in ROS such as with $CoCl_2$ may transiently activate a signaling cascade, leading to induction of HIF1-α. The mechanisms by which $CoCl_2$ leads to increased enzyme activity need further investigation and are beyond the scope of this report. The role of XO in HIF1-α induction in U251-MG cells exposed to $CoCl_2$ was further studied by using siRNA targeted against human XO. siRNA transfection reduced expression of XO in U251-MG and abrogated almost completely $CoCl_2$-induced up-regulation of HIF1-α.

Our observations unequivocally identify a new pathway by which $CoCl_2$-dependent HIF1-α induction in U251-MG cells is mediated by ROS generated by XO. First, $CoCl_2$ allowed the stabilization and nuclear translocation of HIF1-α under normoxic conditions; second, $CoCl_2$ augmented intracellular accumulation of ROS; third, selective antioxidants attenuated $CoCl_2$-mediated activation of HIF1-α; fourth, $CoCl_2$ significantly increased XO activity; fifth, treatment of cells with the XO inhibitor allopurinol blocked ROS generation; sixth, blockade of XO activity abrogated $CoCl_2$-dependent HIF1-α activation; and finally, siRNA targeted against XO reduced expression of XO and significantly reduced HIF1-α accumulation after $CoCl_2$ treatment. Based on our previous definition of bioenergetic phenotypes (19), this pathway mediated by XO is specific to glioma cells that exhibited a glycolytic-dependent phenotype and should confer a major role in controlling HIF1-α regulation in these cells.

To further elucidate the pathways leading to activation of HIF1-α, glutathione concentration was enzymatically assessed in cultures exposed to 5 hours of $CoCl_2$ treatment. We noted that $CoCl_2$ treatment in D54-MG cells resulted in a reduction of [GSH] with a modest increased in [GSSG].

The present investigation has further illuminated the mechanism of action by which $CoCl_2$ mediates its inductive effect on HIF1-α through XO. Taken together, the present study favors a model in which XO-induced generation of ROS leads to the activation of HIF1-α. The finding that HIF1-α is activated via an ROS-sensitive, XO-dependent mechanism points toward a more general role of this transcription factor in tumor progression.

From the experiments shown here, we conclude that ROS were indeed generated in D54-MG cells exposed to $CoCl_2$ but it was unlikely that ROS participated in the hypoxic signal transduction pathways in this cell type. These results are consistent with the result from Salnikow et al. (13). They concluded that ROS production was increased during exposure of A549 cells to nickel or cobalt; however, ROS were not involved in HIF1-α activation. A similar observation was made by Hohler et al. (43) who found that ROS production was increased in PC12 cells during hypoxia but was not the cause of the hypoxia-driven tyrosine hydroxylase mRNA formation. The complexity of HIF1-α regulation by ROS-dependent or other redox-sensitive pathways in different cell types is also underlined by studies in fetal alveolar epithelial cells where NAC increased HIF1-α expression under nonhypoxic conditions (44), as well as by a report showing that redox mechanisms can target discrete regions of the HIF1-α protein (45). It is likely that cell type–dependent and stimulus-dependent factors control ROS dependency or redox sensitivity of HIF1-α. The XO signaling involved in the regulation of HIF1-α expression may involve location-specific redox reactions,

which may require a more oxidizing environment in the cytosol, such as exists in U251-MG cells. Additional work is required to fully clarify these issues. However, one might speculate that the capacity of glioma cells to mount adaptive redox responses to a hypoxia-like environment is determined by the interplay between reduction-oxidation states, cellular compartments, and the glutathione buffering capacity of the cells.

Acknowledgments

Received 9/19/2005; revised 12/6/2005; accepted 12/16/2005.

Grant support: American Brain Tumor Association, U.S. Public Health Service NIH grant P50CA97247 (C.E. Griguer), and NIH research grants HL074391 and HL71189 (J.R. Lancaster, Jr.).

The costs of publication of this article were defrayed in part by the payment of page charges. This article must therefore be hereby marked *advertisement* in accordance with 18 U.S.C. Section 1734 solely to indicate this fact.

References

1. Semenza GL. Hypoxia-inducible factor 1: master regulator of O_2 homeostasis. Curr Opin Genet Dev 1998;8:588–94.
2. Shih SC, Claffey KP. Hypoxia-mediated regulation of gene expression in mammalian cells. Int J Exp Pathol 1998;79:347–57.
3. Huang LE, Gu J, Schau M, Bunn HF. Regulation of hypoxia-inducible factor 1α is mediated by an O_2-dependent degradation domain via the ubiquitin-proteasome pathway. Proc Natl Acad Sci U S A 1998; 95:7987–92.
4. An WG, Kanekal M, Simon MC, Maltepe E, Blagosklonny MV, Neckers LM. Stabilization of wild-type p53 by hypoxia-inducible factor 1α. Nature 1998; 392:405–8.
5. Santore MT, McClintock DS, Lee VY, Budinger GR, Chandel NS. Anoxia-induced apoptosis occurs through a mitochondria-dependent pathway in lung epithelial cells. Am J Physiol Lung Cell Mol Physiol 2002;282: L727–34.
6. Jiang BH, Agani F, Passaniti A, Semenza GL. V-SRC induces expression of hypoxia-inducible factor 1 (HIF-1) and transcription of genes encoding vascular endothelial growth factor and enolase 1: involvement of HIF-1 in tumor progression. Cancer Res 1997;57: 5328–35.
7. Arany Z, Huang LE, Eckner R, et al. An essential role for p300/CBP in the cellular response to hypoxia. Proc Natl Acad Sci U S A 1996;93:12969–73.
8. Zhu H, Bunn HF. Oxygen sensing and signaling: impact on the regulation of physiologically important genes. Respir Physiol 1999;115:239–47.
9. Semenza GL. Perspectives on oxygen sensing. Cell 1999;98:281–4.
10. Fandrey J, Frede S, Jelkmann W. Role of hydrogen peroxide in hypoxia-induced erythropoietin production. Biochem J 1994;303:507–10.
11. Vanden Hoek TL, Becker LB, Shao Z, Li C, Schumacker PT. Reactive oxygen species released from mitochondria during brief hypoxia induce preconditioning in cardiomyocytes. J Biol Chem 1998;273:18092–8.
12. Guillemin K, Krasnow MA. The hypoxic response: huffing and HIFing. Cell 1997;89:9–12.
13. Salnikow K, Su W, Blagosklonny MV, Costa M. Carcinogenic metals induce hypoxia-inducible factor-stimulated transcription by reactive oxygen species-independent mechanism. Cancer Res 2000; 60:3375–8.
14. Brunelle JK, Bell EL, Quesada NM, et al. Oxygen sensing requires mitochondrial ROS but not oxidative phosphorylation. Cell Metab 2005;1:409–14.
15. Chandel NS, McClintock DS, Feliciano CE, et al. Reactive oxygen species generated at mitochondrial complex III stabilize hypoxia-inducible factor-1α during hypoxia: a mechanism of O_2 sensing. J Biol Chem 2000;275:25130–8.
16. Guzy RD, Hoyos B, Robin E, et al. Mitochondrial complex III is required for hypoxia-induced ROS production and cellular oxygen sensing. Cell Metab 2005;1:401–8.
17. Mansfield KD, Guzy RD, Pan Y, et al. Mitochondrial dysfunction resulting from loss of cytochrome *c* impairs cellular oxygen sensing and hypoxic HIF-α activation. Cell Metab 2005;1:393–9.
18. Minchenko A, Leshchinsky I, Opentanova I, et al. Hypoxia-inducible factor-1-mediated expression of the 6-phosphofructo-2-kinase/fructose-2,6-bisphosphatase-3 (PFKFB3) gene. Its possible role in the Warburg effect. J Biol Chem 2002;277:6183–7.
19. Griguer C, Oliva CR, Gillespie GY. Glucose metabolism heterogeneity in human and mouse malignant glioma cell lines. J Neurooncol 2005;74:123–33.
20. Zweier JL, Broderick R, Kuppusamy P, Thompson-Gorman S, Lutty GA. Determination of the mechanism of free radical generation in human aortic endothelial cells exposed to anoxia and reoxygenation. J Biol Chem 1994;269:24156–62.
21. Bass DA, Parce JW, Dechatelet LR, Szejda P, Seeds MC, Thomas M. Flow cytometric studies of oxidative product formation by neutrophils: a graded response to membrane stimulation. J Immunol 1983;130:1910–7.
22. Carter WO, Narayanan PK, Robinson JP. Intracellular hydrogen peroxide and superoxide anion detection in endothelial cells. J Leukoc Biol 1994;55:253–8.
23. Scandalios JG. Oxidative stress: molecular perception and transduction of signals triggering antioxidant gene defenses. Braz J Med Biol Res 2005;38:995–1014.
24. Thorpe GW, Fong CS, Alic N, Higgins VJ, Dawes IW. Cells have distinct mechanisms to maintain protection against different reactive oxygen species: oxidative-stress-response genes. Proc Natl Acad Sci U S A 2004;101:6564–9.
25. Moldeus P, Cotgreave IA, Berggren M. Lung protection by a thiol-containing antioxidant: *N*-acetylcysteine. Respiration 1986;50 Suppl 1:31–42.
26. Li Y, Trush MA. Diphenyleneiodonium, an NAD(P)H oxidase inhibitor, also potently inhibits mitochondrial reactive oxygen species production. Biochem Biophys Res Commun 1998;253:295–9.
27. Fukuda R, Hirota K, Fan F, Jung YD, Ellis LM, Semenza GL. Insulin-like growth factor 1 induces hypoxia-inducible factor 1-mediated vascular endothelial growth factor expression, which is dependent on MAP kinase and phosphatidylinositol 3-kinase signaling in colon cancer cells. J Biol Chem 2002;277:38205–11.
28. Massey V, Komai H, Palmer G, Elion GB. On the mechanism of inactivation of xanthine oxidase by allopurinol and other pyrazolo[3,4-*d*]pyrimidines. J Biol Chem 1970;245:2837–44.
29. Shannon AM, Bouchier-Hayes DJ, Condron CM, Toomey D. Tumour hypoxia, chemotherapeutic resistance and hypoxia-related therapies. Cancer Treat Rev 2003;29:297–307.
30. Prajda N, Weber G. Malignant transformation-linked imbalance: decreased xanthine oxidase activity in hepatomas. FEBS Lett 1975;59:245–9.
31. Ikegami T, Natsumeda Y, Weber G. Decreased concentration of xanthine dehydrogenase (EC 1.1.1.204) in rat hepatomas. Cancer Res 1986;46:3838–41.
32. Kress S, Stein A, Maurer P, et al. Expression of hypoxia-inducible genes in tumor cells. J Cancer Res Clin Oncol 1998;124:315–20.
33. Prajda N, Donohue JP, Weber G. Increased amidophosphoribosyltransferase and decreased xanthine oxidase activity in human and rat renal cell carcinoma. Life Sci 1981;29:853–60.
34. Stirpe F, Ravaioli M, Battelli MG, Musiani S, Grazi GL. Xanthine oxidoreductase activity in human liver disease. Am J Gastroenterol 2002;97:2079–85.
35. Durak I, Beduk Y, Kavutcu M, et al. Activity of the enzymes participating in purine metabolism of cancerous and noncancerous human kidney tissues. Cancer Invest 1997;15:212–6.
36. Biri H, Ozturk HS, Kacmaz M, Karaca K, Tokucoglu H, Durak I. Activities of DNA turnover and free radical metabolizing enzymes in cancerous human prostate tissue. Cancer Invest 1999;17:314–9.
37. Belbin TJ, Singh B, Barber I, et al. Molecular classification of head and neck squamous cell carcinoma using cDNA microarrays. Cancer Res 2002;62: 1184–90.
38. Turrens JF, Alexandre A, Lehninger AL. Ubisemiquinone is the electron donor for superoxide formation by complex III of heart mitochondria. Arch Biochem Biophys 1985;237:408–14.
39. Garcia-Ruiz C, Colell A, Morales A, Kaplowitz N, Fernandez-Checa JC. Role of oxidative stress generated from the mitochondrial electron transport chain and mitochondrial glutathione status in loss of mitochondrial function and activation of transcription factor nuclear factor-κB: studies with isolated mitochondria and rat hepatocytes. Mol Pharmacol 1995;48:825–34.
40. McCord JM. Oxygen-derived free radicals in postischemic tissue injury. N Engl J Med 1985;312:159–63.
41. Marchetti S, Gimond C, Roux D, Gothie E, Pouyssegur J, Pages G. Inducible expression of a MAP kinase phosphatase-3-GFP chimera specifically blunts fibroblast growth and ras-dependent tumor formation in nude mice. J Cell Physiol 2004;199:441–50.
42. Linder N, Martelin E, Lapatto R, Raivio KO. Posttranslational inactivation of human xanthine oxidoreductase by oxygen under standard cell culture conditions. Am J Physiol Cell Physiol 2003; 285:C48–55.
43. Hohler B, Lange B, Holzapfel B, et al. Hypoxic upregulation of tyrosine hydroxylase gene expression is paralleled, but not induced, by increased generation of reactive oxygen species in PC12 cells. FEBS Lett 1999; 457:53–6.
44. Haddad JJ, Olver RE, Land SC. Antioxidant/pro-oxidant equilibrium regulates HIF-1α and NF-κB redox sensitivity. Evidence for inhibition by glutathione oxidation in alveolar epithelial cells. J Biol Chem 2000; 275:21130–9.
45. Lando D, Pongratz I, Poellinger L, Whitelaw ML. A redox mechanism controls differential DNA binding activities of hypoxia-inducible factor (HIF) 1α and the HIF-like factor. J Biol Chem 2000;275:4618–27.

Xanthine Oxidase–Dependent Regulation of Hypoxia-Inducible Factor in Cancer Cells

Corinne E. Griguer, Claudia R. Oliva, Eric E. Kelley, et al.

Cancer Res 2006;66:2257-2263.